




Cite this: *RSC Adv.*, 2021, **11**, 39306

# A novel strategy for sensitive and rapid detection of ascorbic acid *via* the Tyndall effect of cobalt hydroxide nanoflakes†

Qian Gao, Jing Wan, Xuejiang Chen, Xiaomei Mo, Yao Sun, Jianmei Zou, \*  
Jinfang Nie and Yun Zhang \*

Cobalt oxyhydroxide (CoOOH) nanoflakes, as nanoenzymes and fluorescence quenchers, have been widely used in colorimetric and fluorescent analysis. However, their promising light scattering property—the Tyndall effect (TE)—has never been applied in biosensors and biological analysis to date. Herein, we report for the first time a novel strategy for point-of-care detection of ascorbic acid (AA) with the TE of CoOOH nanoflakes providing colorimetric signaling. In this detection system, CoOOH nanoflakes exhibit a strong red TE signal under the illumination of a hand-held 635 nm laser pointer pen. However, the introduction of AA could induce a significant decrease of the TE because it could reduce CoOOH into  $\text{Co}^{2+}$  and results in the degradation of the CoOOH nanoflakes. The changes in the TE intensity could be read-out using a smartphone for the portable quantitative analysis of AA. The results showed that this CoOOH nanoflake-based TE-inspired assay (TEA) exhibited a good linear range from 0.25  $\mu\text{M}$  to 40  $\mu\text{M}$  for AA, with a detection limit of 12 nM. It also showed high selectivity toward AA over common potential interfering species. Importantly, this method possessed the advantages of simple operation, low consumption of time and equipment-free analysis and was successfully applied to the detection of AA in vitamin C tablets.

Received 18th October 2021  
Accepted 2nd December 2021

DOI: 10.1039/d1ra07702c

rsc.li/rsc-advances

## Introduction

Ascorbic acid (vitamin C, AA), as a crucial micronutrient, plays important roles in many metabolic pathways, such as balancing the oxidative stress of the human body and neurotransmitter-related enzyme-involving processes.<sup>1–3</sup> A variety of studies have reported that abnormal levels of AA expression are closely related to various diseases, including scurvy, diarrhea, mental illness, atherosclerosis, cancers and so on.<sup>4–6</sup> Besides, AA, as an important antioxidant, has also been widely used in food, cosmetics and pharmaceutical formulations.<sup>7,8</sup> Therefore, the development of effective method for the detecting AA levels is of great significance for the disease diagnosis, food safety, and cosmetic applications.

Up to now, numerous methods have been proposed for the detection of AA, including enzyme-linked immunosorbent assay,<sup>9</sup> electrochemical sensors,<sup>10</sup> high performance liquid chromatography,<sup>11,12</sup> and so on. Although these methods indeed possess excellent sensing performances, most of them suffer from obstacles such as high cost, requirement for sophisticated

equipment and professional personnel. Therefore, the development of a point-of-care testing (POCT) techniques with the advantages of low-cost, easy handling, equipment-free, high sensitivity and selectivity for sensing AA, is still urgently desired.

Recently, with the advances in nanotechnology, various nanomaterials have been employed for the design of optical nanosensors for the low-cost, rapid detection of AA.<sup>13–16</sup> In 2014, Tang group discovered the specific oxidation–reduction reaction between CoOOH nanoflakes and AA. According to this finding, a CoOOH nanoflakes-modified persistent luminescence nanoparticles-based fluorescent nanoprobe was developed for monitoring AA.<sup>17</sup> After that, a variety of AA optical nanosensors based on the CoOOH nanoflakes has been constructed.<sup>18–20</sup> For examples, Zhang and co-authors reported a two-photon fluorescence nanoprobe for sensing AA in living system by absorbing CoOOH nanoflakes on two-photon nanoparticles.<sup>21</sup> Based on the high oxidisability of CoOOH nanoflakes toward TMB, Li group designed a novel colorimetric strategy for rapid detection of AA.<sup>22</sup> These methods opened new ways in exploring sensing systems for AA. However, in the above methods, CoOOH nanoflakes usually server as nanoenzymes or fluorescence quenchers, and none of them is based on the Tyndall effect (TE) of CoOOH nanoflakes. To the best of our knowledge, the TE of CoOOH nanoflakes, a familiar visible light

College of Chemistry and Bioengineering, Guilin University of Technology, Guilin 541004, P. R. China. E-mail: 2019136@glut.edu.cn; zy@glut.edu.cn; Fax: +86 773 5896839; Tel: +86 773 5896453

† Electronic supplementary information (ESI) available: Supplementary experimental data. See DOI: 10.1039/d1ra07702c



scattering phenomenon of colloidal solutions, has never been applied in colorimetric chemical and biological analysis.

Herein in this work, for the first time, a novel strategy for one-step sensitive, selective, portable detection of AA has been proposed with the TE of CoOOH nanoflakes as colorimetric signaling and CoOOH nanoflakes as AA recognition units. As illustrated in Scheme 1, under the illumination of a hand-held 635 nm laser pointer pen, CoOOH nanoflakes (with 80–120 nm in diameter) produce a strong red TE signal. Upon the addition of AA, the CoOOH nanoflakes were reduced into  $\text{Co}^{2+}$  and the TE of CoOOH nanoflakes decreased significantly due to the decomposing of the CoOOH nanoflakes. In this nanosensor, the TE signaling can be readout by a smartphone to achieve portable quantitative measurement of AA concentration. This method showed high sensitivity to AA with a limit of detection (LOD) of 12 nM. This nanoprobe also exhibited high selectivity to AA over common potential interfering species and has been successfully applied to the detection of AA in vitamin C tablets.

## Experimental

### Reagents and apparatus

Ascorbic acid (AA), sodium hypochlorite (NaClO), cobalt chloride ( $\text{CoCl}_2$ ) and glutathione (GSH) were obtained from Aladdin Chemical Reagent Co., Ltd (Shanghai, China). Sodium hydroxide (NaOH), potassium chloride (KCl), sodium chloride (NaCl), aluminium nitrate ( $\text{Al}(\text{NO}_3)_3$ ), zinc nitrate ( $\text{Zn}(\text{NO}_3)_2$ ), magnesium chloride ( $\text{MgCl}_2$ ) and copper chloride ( $\text{CuCl}_2$ ) were purchased from Xilong Chemical Co., Ltd (Guangzhou, China). D-Glucose (D-Glu), L-histidine (L-His), L-serine (L-Ser), L-alanine (L-Ala), L-valine (L-Val), L-threonine (L-Thr), L-tyrosine (L-Tyr), L-proline (L-Pro), L-leucine (L-Leu), L-arginine (L-Arg), lysine (Lys) and glycine (Gly) were bought from Shanghai Hualan Chemical Technology Co., Ltd (Shanghai, China). All other chemicals were of analytical grade and used as received without further purification. Unless stated otherwise, all stock solutions were prepared with deionized water (specific resistivity  $\geq 18.2 \text{ M}\Omega \text{ cm}$ ) produced from an ultrapure water system (UPS-II-20L) that was from Chengdu Yuechun Technology Co., Ltd. (Chengdu, China).

Optical characterization of the CoOOH nanoflakes treated with or without AA was performed on a UV-vis spectrometer (Cary 50, Varian, USA). The Fourier transform infrared spectra (FT-IR) were measured within the  $4000\text{--}500 \text{ cm}^{-1}$  region on an infrared spectrophotometer (Nicolet iS10, Thermo, USA). Scanning electron microscope (SEM, EVO18, Zeiss, Germany) were applied for the morphological investigation of the CoOOH nanoflakes. Hydrated particle size and zeta potential of the CoOOH nanoflakes were measured using a Zetasizer Nano (Zetasizer Nano ZS90, Malvern Instruments Ltd., UK) at room temperature. TE signals was produced using a handheld light source, *i.e.*, a 635 nm red laser pointer pen (5 mW) was bought from Deli Group Co., Ltd. (Ningbo, China). Images of all colorimetric results were recorded by a smartphone (Xiaomi 6A).

### Preparation of CoOOH nanoflakes

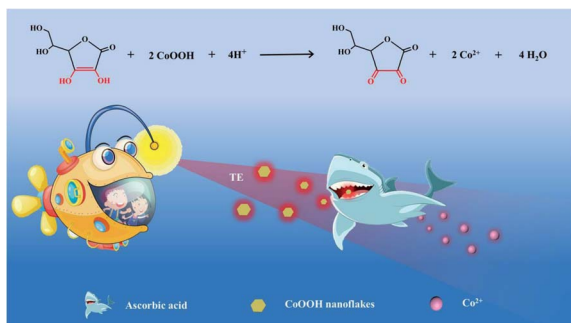
The CoOOH nanoflakes were synthesized based on the previous method with slight modifications.<sup>23</sup> In brief; 5 mL of NaOH (0.8 M) solution was added dropwise into 5 mL of  $\text{CoCl}_2$  (10 mM) with vigorous stirring. After stirring for 5 minutes, the mixture was sonicated for another 5 minutes. Subsequently, 5 mL of NaClO (0.2 M) was added to the above solution, and the resulting suspension kept stirring for another 30 min. The final solid product was collected by centrifugation at 8000 rpm for 5 min, then washed with ultrapure water for three times. The resulting CoOOH nanoflakes were dried using a freeze dryer and stored in a dry environment for further use.

### TE signaling method for AA detection

For the TE signaling method, CoOOH nanoflakes solution ( $2.5 \mu\text{g mL}^{-1}$ ) was diluted by the deionized water, and different concentrations (0, 0.25, 0.5, 1.25, 2.5, 5, 12.5, 20, 40, 60, 80  $\mu\text{M}$ ) of AA were added to the solution at room temperature. After incubation of 12 min, the TE signal of the resulting mixture was produced with the illumination of the portable red laser pointer pen. For quantitative analysis, TE images of all samples were captured by smartphone and its average gray (AG) value was measured using the ImageJ processing software. The  $\Delta\text{AG}$  value for each AA sample was defined as  $\Delta\text{AG} = \text{AG}_0 - \text{AG}$ , where  $\text{AG}_0$  and AG were obtained from the CoOOH nanoflakes solution treated without or with AA sample, respectively. Specificity experiments were performed in the same manner but using  $\text{K}^+$ ,  $\text{Na}^+$ ,  $\text{Al}^{3+}$ ,  $\text{Zn}^{2+}$ ,  $\text{Mg}^{2+}$ ,  $\text{Cu}^{2+}$ ,  $\text{Co}^{2+}$ , D-Glu, GSH, L-His, L-Ser, L-Ala, Lys, L-Val, L-Thr, Gly, L-Tyr, L-Pro, L-Leu, L-Arg instead of AA.

### Surface plasmon resonance (SPR) signaling method for AA detection

For the traditional SPR-based method, CoOOH nanoflakes solution ( $250 \mu\text{g mL}^{-1}$ ) was diluted by the deionized water, and different concentrations (0, 10, 20, 40, 60, 80, 150, 200, 300, 500  $\mu\text{M}$ ) of AA were added to the solution at room temperature. After incubation of 10 min, the UV-vis spectrum for each reaction mixture was recorded for further quantitative measurement.



**Scheme 1** Schematic illustration of the working principle of CoOOH nanoflakes-based TEA method for sensitive and portable detection of AA.



## Results and discussion

In this TE-inspired assay (TEA), CoOOH nanoflakes acted as both AA recognition units and TE reporters. The CoOOH nanoflakes were synthesized *via* a redox reaction between CoCl<sub>2</sub> and NaClO according to the previous report.<sup>23</sup> The obtained CoOOH nanoflakes solution show a yellowish-brown color in aqueous solution, while the CoCl<sub>2</sub> solution was pink (inset of Fig. 1A). Compared to the absorption band of CoCl<sub>2</sub> (~510 nm), the absorption band of CoOOH nanoflakes exhibited a maximum absorption peak at 418 nm (Fig. 1A), which is similar to that in the previous literature. The morphology of CoOOH nanoflakes was characterized with SEM and the results indicated that the CoOOH nanoflakes were hexagonal plate shape with average size of 120 nm (Fig. 1B). Simultaneously, the DLS results show that CoOOH nanoflakes presented uniform hydrodynamic size (120 nm) with a particle dispersion index (PDI) of 0.172 (Fig. S1†) and the zeta potential of them was 12.4 mV (Fig. S2†). The FT-IR spectrum of CoOOH nanoflakes in the range of 500–4000 cm<sup>-1</sup> show that the characteristic absorption bands are located at 3434 cm<sup>-1</sup> (hydroxyl group), 1628 cm<sup>-1</sup> (Co–O) and 582 cm<sup>-1</sup> (Co–O<sup>2-</sup>), which were consistent with previous reports (Fig. 1C).<sup>24</sup> Besides, the XRD patterns of CoOOH nanoflakes exhibited several diffraction peaks corresponding to the rhombohedral heterogenite structure, which confirms that these materials are pure CoOOH nanoflakes (Fig. 1D).<sup>25</sup> All of the above results indicated the successful preparation of CoOOH nanoflakes.

Having demonstrated the successful synthesis of the CoOOH nanoflakes, the feasibility of the AA-induced degradation of CoOOH nanoflakes with a decreased TE response was then investigated. As shown in Fig. 2A, a freshly-prepared solution containing CoOOH nanoflakes exhibited a strong absorption at 418 nm in the UV-vis spectrum with a yellowish-brown color

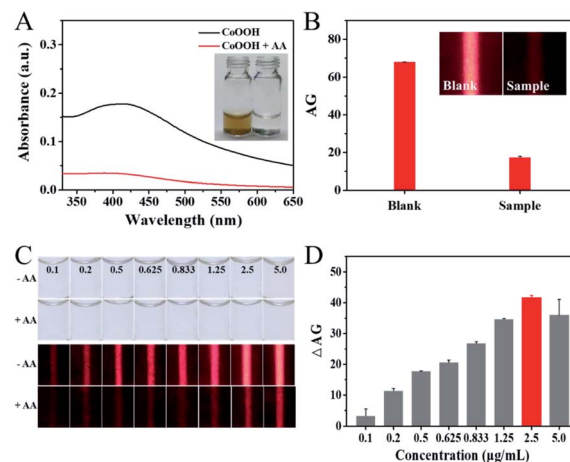


Fig. 2 (A) UV-vis absorption spectrum of the CoOOH nanoflakes solution treated with (red line) or without AA (black line). Inset shows the corresponding photograph of reaction solutions. (B) The corresponding average grayscale (AG) results of the TE images shown in inset. Inset shows TE results obtained from the CoOOH nanoflakes solution treated with (right) or without AA (left). (C) Optical images of the CoOOH nanoflakes at different concentrations (0.1, 0.2, 0.5, 0.625, 0.833, 1.25, 2.5, 5.0 µg mL<sup>-1</sup>) and the corresponding TE images obtained from the above solution treated without or with 10 µM AA samples. (D) The average grayscale change (ΔAG) of the TE images shown in (C).

(inset of Fig. 2A). However, after addition of the AA into the above solution, the yellowish-brown color of CoOOH nanoflakes faded and the absorption intensity of the 418 nm band sharply decreased. This may be attributed to the specific redox reaction between the CoOOH nanoflakes with the enediol group of AA, which could result in the reduction of CoOOH nanoflakes to Co<sup>2+</sup> in the presence of AA. More importantly, the dispersed CoOOH nanoflakes with hydrodynamic size of 120 nm showed a strong TE signal (inset of Fig. 2B) under the irradiation of the 635 nm red laser pointer, which could be dramatically decreased *via* their degradation by the introduction of AA. An obvious difference between average gray (AG) values of the TE signals recorded from the CoOOH nanoflakes treated with or without AA was also shown in Fig. 2B. Thus, the above results indicated well the feasibility of AA-adjusted TE signals of the CoOOH nanoflakes.

Having confirmed the feasibility of this novel method, several reaction conditions were then optimized to achieve the best analytical performance for AA detection. Firstly, the effect of the concentration of CoOOH nanoflakes on the TE response of the nanosensor was investigated (Fig. 2C and D). It can be found that when the CoOOH nanoflakes level decreases from 5.0 to 0.1 µg mL<sup>-1</sup>, all of the solution is completely colorless, which indicated that the surface plasmon resonance (SPR) property of them can be negligible. However, the clear TE signals could be observed in all of the above solution and the obvious TE signal changes of them could be obtained by incubating with AA. In other words, the TE of CoOOH nanoflakes might offer a more ideal colorimetric signaling efficiency over the most widely applied SPR method to achieve a naked-eye

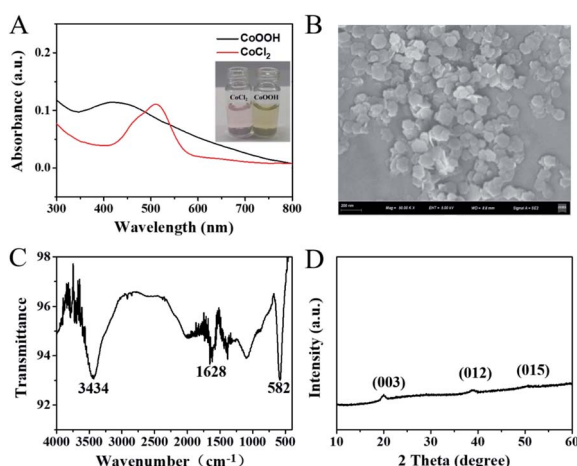


Fig. 1 (A) UV-vis absorption spectra of CoOOH nanoflakes (50 µg mL<sup>-1</sup>, black curve) and CoCl<sub>2</sub> solution (20 µM, red curve), respectively. Inset: digital images of CoCl<sub>2</sub> solution (left) and CoOOH nanoflakes (right). (B) SEM image of the CoOOH nanoflakes. (C) FT-IR spectrum of CoOOH nanoflakes. (D) The X-ray diffraction pattern of CoOOH nanoflakes.





analysis of AA. The maximal average grayscale change ( $\Delta AG$ ) can be observed when the concentration of CoOOH nanoflakes is  $2.5 \mu\text{g mL}^{-1}$  and this concentration was chosen as the optimal condition for the further experiments.

Then, the kinetic response of this sensing system for AA detection has been studied. After incubation of AA with CoOOH nanoflakes for different time (1, 4, 8, 12, 16 and 20 minutes), the TE signals of mixtures were recorded. As shown in Fig. S3,<sup>†</sup> the  $\Delta AG$  increases gradually until reaching an equilibrium at 12 min and it was chosen for the following experiments. This result also stated that this sensing platform for AA detection exhibited fast response ability, which makes this assay possess the potential for point-of-care testing. In addition, the temperature for the reactions between the CoOOH nanoflakes and AA samples was also investigated. It has been found that the maximal  $\Delta AG$  was obtained at  $25^\circ\text{C}$  (Fig. S4<sup>†</sup>) and it was chosen for further investigation.

Under the optimized experimental conditions, the sensing performance of CoOOH nanoflakes-based TEA was evaluated by testing AA in the range from 0 to  $80 \mu\text{M}$ . The results showed that all of the CoOOH nanoflakes solution exhibited nearly-colorless (Fig. 3A, top, images 1–11), which could be attributed to the fact that the amount of CoOOH nanoflakes ( $2.5 \mu\text{g mL}^{-1}$ ) were too low to produce visual SPR-related color responses in solution. For the same reason, the absorption observed in their UV-vis spectrum was negligible (Fig. 3C, red curve A1–A11). However, obvious TE signals could be obtained in most of these colorless mixtures under the illumination of the hand-held red laser pointer and the TE single intensity decreased gradually (Fig. 3A, bottom) with the AA concentration increased. As shown in Fig. 3D, the red calibration curve described the relationship

between the  $\Delta AG$  values and the logarithm values of AA concentrations ( $\log C_{AA}$ ) and a good linear correlation ( $y = 15.0329x - 35.3039$ ,  $R^2 = 0.9992$ , red dots) from 0.25 to  $40 \mu\text{M}$  with a LOD of 12 nM was obtained ( $3\sigma$ ). Comparing with TEA method, a larger amount of CoOOH nanoflakes ( $250 \mu\text{g mL}^{-1}$ ) need to be consumed to analyze the samples with different AA concentrations by the SPR-based approach ( $y = 0.4308x - 1.9434$ ,  $R^2 = 0.9872$ , black dots). The AA-induced CoOOH nanoflakes' degradation made the color of reaction mixture gradually change from yellowish-brown to colorless (Fig. 3B). The results (Fig. 3C, black curve Ba–Bk) showed that the absorbance intensity in the UV-vis spectra recorded at 418 nm ( $A_{418}$ ) of the above reaction mixtures gradually decreased and the values of  $\Delta A$  ( $A_0 - A$ ) exhibited a good linear relationship to the AA concentration ( $40\text{--}300 \mu\text{M}$ ). However, the LOD achieved by the traditional SPR method ( $1.05 \mu\text{M}$ ) is 87.5 times higher than that obtained from the TE method. In addition, comparing with recent nanoprobe-based colorimetric technology with a UV-vis spectrometer as the quantitative reader, this CoOOH nanoflakes-based TE sensor just requires a cheap laser pointer pen and a smartphone to achieve rapid and portable quantification of AA with comparable or even better analytical sensitivity (Table S1<sup>†</sup>).

Besides sensitivity, selectivity is another important parameter to evaluate the performance of a newly developed nanosensor. To evaluate the selectivity of the CoOOH nanoflakes-based TEA for AA, the TE signals from the mixing of the CoOOH nanoflakes solution and various potentially competing interfering agents were recorded and the corresponding average grayscale (AG) was calculated as an evaluation standard. As shown in Fig. 4, a significant change of TE signal intensity can be found in the presence of AA, while the other interferences do not lead to obvious TE signal intensity change. Thus, this CoOOH nanoflakes-based TEA possess a good selectivity for AA detection and could be applied to practical complex samples analysis.

To evaluate the applicability of this developed strategy in real samples, AA level in vitamin C tablets was studied (Table S2<sup>†</sup>). The recovery values of AA in real Vitamin-C tablet samples are in the range of 94.3–104.2%, and the relative standard deviations (RSDs) are between 3.10 and 7.71% ( $n = 3$ ). These data indicates

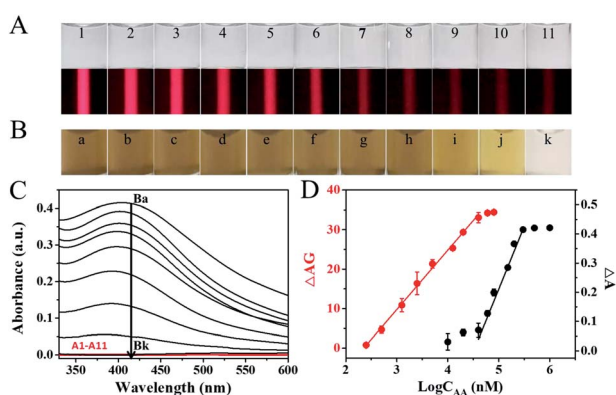


**Fig. 3** (A) Colorimetric (top) and TE (bottom) results obtained from the mixing of CoOOH nanoflakes ( $2.5 \mu\text{g mL}^{-1}$ ) and AA of different concentrations: (1) 0, (2) 0.25, (3) 0.5, (4) 1.25, (5) 2.5, (6) 5, (7) 12.5, (8) 20, (9) 40, (10) 60 and (11)  $80 \mu\text{M}$ . (B) Colorimetric (top) results obtained from the mixing of CoOOH nanoflakes ( $250 \mu\text{g mL}^{-1}$ ) and AA of different concentrations: (a) 0, (b) 10, (c) 20, (d) 40, (e) 60, (f) 80, (g) 150, (h) 200, (i) 300, (j) 500 and (k)  $1000 \mu\text{M}$ . (C) UV-vis spectra measured from the reaction mixtures shown in (A) (red curves A1–A11) and (B) (black curves Ba–Bk). (D) Calibration curves describing the relationships between the average grayscale change ( $\Delta AG$ ) of the TE shown in (A) (red curves) or  $A_0 - A$  values recorded at 418 nm in UV-vis spectrum (black curves) and the logarithm values of the AA concentrations ( $\log C_{AA}$ ).

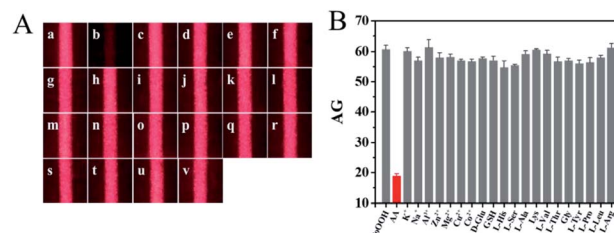


**Fig. 4** (A) TE images obtained from the reactions of the  $2.5 \mu\text{g mL}^{-1}$  CoOOH nanoflakes solutions and  $50 \mu\text{M}$  AA, other potential interferences ( $500 \mu\text{M}$  each). (B) The corresponding average grayscale (AG) results of the TE images shown in (A). Each error bar represents a standard deviation across three replicate experiments.



that this CoOOH nanoflakes-based TE-inspired assay is feasible and reliable for monitoring AA in real samples.

## Conclusions

In this work, a novel CoOOH nanoflakes-based TEA method has been developed for the one-step sensitive, selective and portable determination of AA. In this nanosystem, the CoOOH nanoflakes solution exhibits strong TE signal under the illumination of a laser pointer. However, the TE of CoOOH nanoflakes solution significantly decreases in the presence of AA, because it efficiently reduces CoOOH into  $\text{Co}^{2+}$  and results in the degradation of the CoOOH nanoflakes, which affords a highly sensitive detection of AA in aqueous solutions with a LOD of 12 nM. More importantly, this equipment-less method only requires a laser pointer and a smartphone but powerful computing capabilities to implement simple, rapid, selective and portable quantitative analysis. We anticipate that CoOOH nanoflakes-based TE colorimetric methodology hold great potential to develop a simple and sustainable technology for point-of-care detection of AA.

## Conflicts of interest

The authors declare no competing financial interest.

## Acknowledgements

This work was financially supported by Natural Science Foundation of Guangxi Province (No. 2020GXNSFBA297114), National Natural Science Foundation of China (No. 21874032, 21765007 and 21765005), Guangxi Key Research Project (No. GuikeAB17129003), Guangxi Science Fund for Distinguished Young Scholars (No. 2018GXNSFFA281002), Central Government-Guided Local Science and Technology Development Project (No. GuikeZY20198006), and Guangxi Graduate Education Innovation Plan (No. YCSW2020170).

## References

- 1 S. J. Padayatty, H. D. Riordan, S. M. Hewitt, A. Katz, L. J. Hoffer and M. Levine, *Can. Med. Assoc. J.*, 2006, **174**, 937–942.
- 2 H. Liu, W. Na, Z. Liu, X. Chen and X. Su, *Biosens. Bioelectron.*, 2017, **92**, 229–233.

- 3 K. Liu, P. Yu, Y. Lin, Y. Wang, T. Ohsaka and L. Mao, *Anal. Chem.*, 2013, **85**, 9947–9954.
- 4 D. Farbstein, A. Kozakblikstein and A. P. Levy, *Molecules*, 2010, **15**, 8098.
- 5 Y. Umasankar, U. Yogeswaran, S. Thiagarajan and S. M. Chen, *Anal. Biochem.*, 2007, **365**, 122–131.
- 6 M. A. Esteban and D. Pei, *Nat. Genet.*, 2012, **44**, 366.
- 7 J. Liu, Y. Chen, W. Wang, J. Feng, M. Liang, S. Ma and X. Chen, *J. Agric. Food Chem.*, 2016, **64**, 371–380.
- 8 S. Rumsey and M. Levine, *J. Nutr. Biochem.*, 1998, **9**, 116–130.
- 9 S. Uchiyama, Y. Kobayashi, S. Suzuki and O. Hamamoto, *Anal. Chem.*, 1991, **63**, 2259–2262.
- 10 K. Deng, X. Li and H. Huang, *Microchim. Acta*, 2016, **183**, 2139–2145.
- 11 D. R. Lima, M. Cossenza, C. G. Garcia, C. C. Portugal, F. F. d. C. Marques, R. Paes-de-Carvalho and A. D. P. Netto, *Anal. Methods*, 2016, **8**, 5441–5447.
- 12 R. Shakya and D. A. Navarre, *J. Agric. Food Chem.*, 2006, **54**, 5253–5260.
- 13 W. Huang, Y. Deng and Y. He, *Biosens. Bioelectron.*, 2016, **91**, 89–94.
- 14 Y. J. Chen and X. P. Yan, *Small*, 2009, **5**, 2012–2018.
- 15 J. J. Liu, Z. T. Chen, D. S. Tang, Y. B. Wang, L. T. Kang and J. N. Yao, *Sens. Actuators, B*, 2015, **212**, 214–219.
- 16 M. Zheng, Z. Xie, D. Qu, D. Li, P. Du, X. Jing and C. Zai, *ACS Appl. Mater. Interfaces*, 2013, **5**, 13242–13247.
- 17 N. Li, Y. Li, Y. Han, W. Pan, T. Zhang and B. Tang, *Anal. Chem.*, 2014, **86**, 3924–3930.
- 18 L. Li, C. Wang, K. Liu, Y. Wang, K. Liu and Y. Lin, *Anal. Chem.*, 2015, **87**, 3404–3411.
- 19 Q. Han, H. Yang, S. Wen, H. Jiang, L. Wang and W. Liu, *Inorg. Chem. Front.*, 2018, **5**, 773–779.
- 20 H. Xu, Q. Cai, Q. Nie, Z. Qiao, S. Liu and Z. Li, *RSC Adv.*, 2018, **8**, 23720–23726.
- 21 H. M. Meng, X. B. Zhang, C. Yang, H. Kuai, G. J. Mao, L. Gong, W. Zhang, S. Feng and J. Chang, *Anal. Chem.*, 2016, **88**, 6057–6063.
- 22 D. Ji, Y. Du, H. Meng, L. Zhang, Z. Huang, Y. Hu and Z. Li, *Sens. Actuators, B*, 2018, **256**, 512–519.
- 23 S. G. Liu, L. Han, N. Li, N. Xiao, Y. J. Ju, N. B. Li and H. Q. Luo, *J. Mater. Chem. B*, 2018, **6**, 2843–2850.
- 24 L. Li, C. Wang, K. Liu, Y. Wang, K. Liu and Y. Lin, *Anal. Chem.*, 2015, **87**, 3404–3411.
- 25 J. Yang and T. Sasaki, *Chem. Mater.*, 2008, **20**, 2049–2056.

